

Spatial Disparities in Fire Shelter Accessibility: Capacity Challenges in the Palisades and Eaton Fires

Su Yeon Han^a, Yubin Lee^a, Jooyoung Yoo^b, Jeon-Young Kang^c, Jinwoo Park^c, Soe W. Myint^d, Eunsang Cho^e, Xin Gu^a, Joon-Seok Kim^{f,*}

^a*Department of Geography and Environmental Studies, Texas State University, 601 University Drive, San Marcos, 78666, TX, USA*

^b*Spatial Sciences Institute, University of Southern California, Crocker Plaza, 3616 Trousdale Parkway, Los Angeles, 90089, CA, USA*

^c*Department of Geography, Kyung Hee University, 26 Kyunghaedae-ro, Dongdaemun-gu, Seoul, 02447, Republic of Korea*

^d*The Meadows Center for Water and the Environment, Texas State University, 601 University Drive, San Marcos, 78666, TX, USA*

^e*Ingram School of Engineering, Texas State University, 601 University Drive, San Marcos, 78666, TX, USA*

^f*Department of Computer Science, Emory University, 400 Dowman Drive, Atlanta, 30322, GA, USA*

Abstract

The increasing frequency and severity of wildfire in California, exacerbated by prolonged drought and environmental changes, pose significant challenges to urban community resilience and equitable emergency response. The study investigates issues of accessibility to shelters during the Palisades and Eaton Fires which started in January 2025 in Southern California that led to over 180,000 displacements and the loss of 16,000 structures. Despite coordinated efforts of many organizations' emergency assistance, shelter shortages left many evacuees without safety or accessible refuge. This research aims to measure shelter accessibility during the fires' peak, evaluate whether existing shelter capacity met the demand, and identify spatial disparities in access. Results reveal severe shelter shortages and pronounced inequities in access to shelters, particularly in geographically isolated regions and mountainous areas. Our simulations of shelter placement strategies using a capacity-based algorithm and a proximity-based approach demonstrate potential improvements in both shelter accessibility and equitable access to shelters. The findings underscore the critical need

*Corresponding author

Email address: joonseok.kim@emory.edu (Joon-Seok Kim)

for strategic shelter planning and infrastructure development to enhance disaster readiness and reduce vulnerability in regions that frequently experience wildfires.

Keywords: spatial accessibility, wildfire, disparities, shelter, simulation

1. Introduction

The western United States has experienced more frequent wildfires in recent years with California particularly at risk due to prolonged drought conditions and increased temperatures [1, 2, 3, 4]. The growing intensity of wildfires has resulted in disastrous consequences by claiming lives, destroying property, and damaging essential public infrastructure including roads, power, and water systems. [5, 6, 7, 8]. On January 7, 2025, the Palisades and Eaton Fires began in Southern California. The Palisades Fire in Los Angeles spread to a size of 23,700 acres by January 12 [9], while the Eaton Fire near Pasadena expanded to over 14,000 acres within several days [10]. The Palisades and Eaton Fires continued for 24 days until they were completely contained by January 31, 2025 [11]. The extensive burning period of the Palisades and Eaton Fires led to widespread devastation—the Palisades Fire destroyed 7,000 structures and resulted in 12 fatalities, while the Eaton Fire crushed more than 9,000 structures and claimed 17 lives [12].

The Palisades and Eaton wildfires forced a large number of residents to evacuate, leading to overcrowded shelters and leaving many without immediate refuge. *The New York Times* reported that many of them struggled to find shelters during their evacuations [13]. As part of the response efforts, aid organizations such as the American Red Cross established eight emergency shelters throughout Los Angeles County to help with wildfire evacuations [13]. However, the available facilities were insufficient to accommodate the massive demand, which resulted in many evacuees seeking accommodations from relatives and friends or sleeping in their vehicles [13]. Others attempted to find hotel rooms or short-term rentals but faced difficulties due to a drastic surge in rental demand caused by the massive influx of displaced people [13]. These prolonged shelter shortages forced them to relocate multiple times during the crisis [14]. Access to shelters was particularly limited in geographically isolated areas and settlements on undulating terrains. Specifically, restricted road access and steep terrain were major factors that delayed prompt evacuations [15, 16]. These geographic barriers were especially evident in communities such as the Santa Monica Mountains, where narrow roads restricted both evacuation routes and emergency response operations [17].

The immense destruction and chaos caused by the Palisades and Eaton wildfires highlighted not only the significant financial losses but also the urgent necessity for

better disaster readiness and response systems. The wildfires' aftermath showed the overwhelming extent of destruction, with more than 16,000 structures destroyed which surpassed \$250 billion in economic loss [18]. Beyond the immediate devastation, these wildfires revealed fundamental problems in evacuation planning, shelter accessibility, and resource allocation, underscoring the need for improvement to address the increasing difficulty of disaster management during periods of more frequent natural hazards. One of the most crucial concerns is that many evacuees faced multiple relocations due to the shortage of shelter capacity and insufficient accessibility to shelters [14]. The Palisades and Eaton Fires serve as a reminder that without significant improvements in emergency response systems—particularly in shelter accessibility—a disaster event will create prolonged displacement and hardship.

Although significant challenges to shelter accessibility arose during the Palisade and Eaton Fires, spatial disparities in shelter availability have not been thoroughly examined. Hence, this research aims to investigate shelter accessibility during the crisis while assessing whether they provided sufficient capacity to accommodate evacuees. Additionally, it examines whether evacuees had equitable access to shelters in different regions, while also exploring how geographic differences in shelter accessibility were shaped by traffic congestion during the fire events. Furthermore, this research suggests potential new shelter locations that could improve overall accessibility and ensure more equitable shelter access throughout all evacuation zones. Results and findings from this research can assist shelter placement and distribution of critical resources to better support for displaced populations during future wildfire emergencies.

This research is intended to answer research questions below.

- Q1. How effective was shelter accessibility during the peak of the Palisades and Eaton Fires, and did the total shelter capacity adequately support the displaced population?
- Q2. What were the travel times to the nearest shelters for evacuees, and how did traffic congestion impact spatial accessibility and affected disparities in shelter access?
- Q3. How did shelter accessibility vary across different regions, and to what extent did spatial disparities exist in terms of equitable access to shelters?
- Q4. How can the strategic placement of new shelters improve overall accessibility and ensure equitable shelter access across all regions during disasters?

2. Related Work

Related studies on wildfire evacuations and shelter accessibility fall into three main directions. The first explores the ongoing debate on whether evacuation always enhances safety or, in some cases, may inadvertently increase risk. The second focuses on the difficulties people face when trying to reach shelters located in regions with constrained space. The third extends its analysis beyond wildfires to measure shelter accessibility throughout multiple disaster situations.

Surviving wildfires entails two principal strategies which include evacuation and shelter-in-place (SIP) [19]. Experts generally agree that prompt evacuation is the most effective strategy for reducing fatalities and injuries [20]. When adequate time is available, moving out of the fire affected area can give the greatest chance of survival [21]. However, when active flames block escape routes or the fire advances too quickly, evacuation can potentially be riskier than sheltering in place due to the risk of encountering active flames [22]. In such cases, SIP serves as a last-resort option, potentially providing a higher chance of survival than taking the dangerous evacuation route. This strategy includes seeking refuge in well-prepared, fire-resistant structures [23] or designated safety zones, such as cleared areas with minimal hazards [24, 25]. In extreme situations, people should seek refuge in water bodies to reduce heat exposure [21]. Cova et al. [21] emphasized that no single strategy guarantees safety in wildfire-prone regions, but evacuation remains the most effective option whenever it is feasible.

Research shows that social and geographic inequalities in access to emergency shelters limit disaster response effectiveness and place vulnerable populations at greater risk. Ermagun et al. (2024) noted that the elderly, individuals with disabilities, and Hispanic communities are at greater risk due to limited shelter access [26]. Moreover, geographic disparities create extra challenges for suburban and rural areas, which often struggle with sparse and insufficient emergency facilities [26, 27, 28].

Beyond existing shelter limitations, road network constraints create additional challenges to evacuation efforts. Evacuees' ability to reach safety is hindered by sudden road blockages and fire-related damage to transportation networks [29, 30, 31]. The presence of these barriers not only delays evacuation times but also increases the likelihood of individuals becoming trapped within dangerous zones. As a result, effective evacuation planning and shelter accessibility are critical for mitigating wildfire risks and ensuring equitable access to emergency resources [30].

Beyond general evacuation concerns, scholars have recently noted that spatial accessibility has become an essential consideration for researchers working on emergency evacuation planning [30]. While accessibility methodologies have been extensively applied in healthcare research, including studies on access to hospitals,

physicians, and preventive care services [32, 33, 34, 35, 36, 37, 38], research on shelter accessibility during disaster evacuations has received less attention. In terms of shelter accessibility research, floating catchment area (FCA) framework—including the two-step floating catchment area (2SFCA) method, its various modifications, and enhanced versions—has been used to assess spatial accessibility in disaster scenarios, though not specifically for wildfires [39, 40, 41, 42, 43, 27, 44]. These approaches combine essential elements, such as road network travel speed(traffic) with shelter capacity(supply) and detailed population (demand) data to analyze spatial access to emergency shelters effectively.

Although studies on emergency shelters’ spatial accessibility have increased, there are still few that are especially focused on wildfires. For example, Ermagun and Janatababi [26] measured accessibility to wildfire shelters but did not account for the dynamic interactions among supply (shelters), demand (population), and travel time—key factors incorporated in the Floating Catchment Area (FCA) framework. Furthermore, the majority of current studies evaluate spatial accessibility to urban emergency facilities such as shelters, fire stations, and emergency centers (e.g., [39, 45, 46, 47, 48]), while often overlooking spatial accessibility in wildfire-prone regions. The populations in these areas are typically scattered throughout forested landscapes and have limited road infrastructure, which complicates emergency response efforts and shelter accessibility. Filling these research gaps will play a crucial role in enhancing wildfire disaster preparedness and ensuring equitable shelter access.

This research contributes to the field by analyzing spatial accessibility to shelters. Building upon prior research—where studies on shelter accessibility in disaster evacuations remain relatively scarce—this research applies advanced spatial accessibility methods to measure shelter accessibility during the Palisades and Eaton Fires. Specifically, the Enhanced Two-Step Floating Catchment Area (E2SFCA) method is employed to evaluate both supply-side factors (e.g., shelter capacity, available facilities) and demand-side dynamics (e.g., evacuee population distribution, mobility constraints). By integrating these critical factors, this study aims to offer new insights into improving shelter accessibility and emergency response strategies for future wildfire events.

3. Study Area and Data

Our study area covers the regions where the Palisades and Eaton fires occurred (Figure 1). Data on wildfire perimeters, evacuation orders, warning zones, and shelter statuses were collected via web crawling from CAL FIRE’s website (fire.ca.gov), which provided frequent updates during active fire periods. According to their live

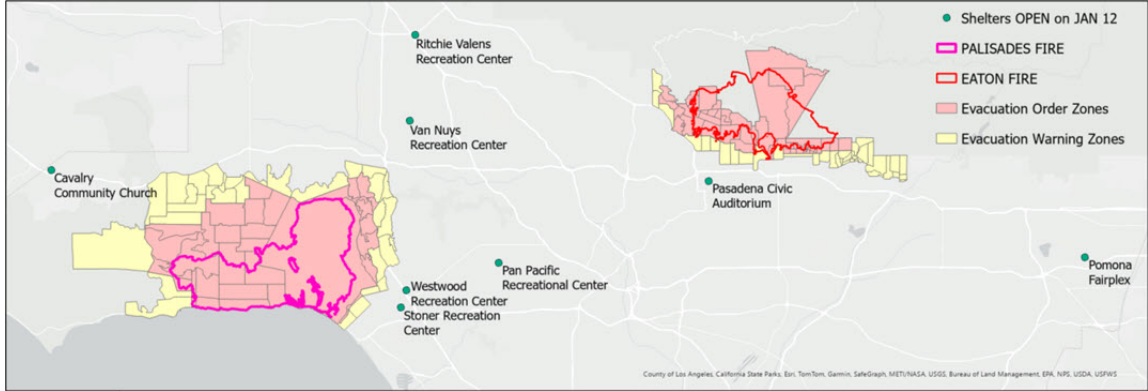


Figure 1: Study area

updates, the Palisades Fire ignited around 10:30 a.m. in the Pacific Palisades neighborhood and expanded to over 11,000 acres by mid-January 8, eventually consuming approximately 23,713 acres. In contrast, the Eaton Fire ignited later on January 7 in the evening at Eaton Canyon near Altadena and expanded rapidly overnight to about 10,600 acres by January 8, eventually burning approximately 14,021 acres by January 16. CAL FIRE’s live updates indicated that the Eaton Fire’s perimeter peaked at 23,713.39 acres on January 12. However, later reports published on January 23, 2025, revised the burned area to 23,448 acres, with notes indicating it is under investigation [49]. Both fires were fully contained on January 31, 2025.

Figure 1 illustrates the locations of each wildfire along with the corresponding evacuation and warning zones and shelter information as of January 12, 2025, the day we focus on examining shelter accessibility. We selected January 12 because, according to CAL FIRE’s live reports, it was the date when the active wildfire expanded to its largest size. Additionally, this date represents an early stage of fire progression when displaced individuals were experiencing significant chaos due to quickly spreading fires that had begun only a few days earlier. At that time, many evacuees did not have clear information about the fire’s trajectory and the extent of its impact, which made shelter accessibility an important concern.

3.1. Shelter Capacity

We gathered the locations, addresses, and overnight counts of available shelters as of January 12, 2025, from the Cal OES News website [50]. The capacity of shelters open on January 12, 2025, as well as other potential shelters used in this study, was collected from the website, National Shelter System Facilities (NSSF) [51]. The dataset includes 70,317 facilities across the U.S. that can accommodate individuals

during an evacuation. While the downloaded shelter data included evacuation capacity information, this information was not consistently available for all shelters. Even though there were 11 shelters that remained open throughout the active Palisades and Eaton fires (as shown in Table 1), capacity information was available for only six of them. For the remaining five shelters, we estimated capacity by assessing the available indoor space using various online sources. For instance, the Van Nuys/Sherman Oaks Recreation Center was found to have approximately 15,000 square feet of space, based on information obtained from a website [52]. We then calculated the usable shelter space according to FEMA guidelines.

FEMA’s Guidelines for Mass Care Shelter Operations (FEMA P-785) specify that non-occupiable areas must be accounted for when planning emergency shelter space [53]. Similarly, the Sphere Handbook implies that only about 65–75% of the total indoor area is usable for sheltering, with approximately 25–35% allocated to non-occupiable spaces such as hallways, mechanical rooms, and storage areas [54]. Based on these recommendations, we assumed that 70% of each facility’s total space was suitable for sheltering. Additionally, we assumed that each person required 100 square feet to ensure a desirable shelter environment. This estimate is based on CDC guidelines, which recommend a minimum of 60 square feet per person in evacuation shelters [55]. However, FEMA further advises that shelters should provide one toilet for every 20 people and one shower for every 25 people. Since no detailed information was available regarding the number of toilets or showers in each shelter facility, we adopted a more conservative estimate of 100 square feet per person to account for potential limitations. A detailed breakdown of how capacity was estimated for each of the five shelters is provided in Appendix A. Table 1 shows all eleven shelter locations and capacities during the Palisades and Eaton wildfires. For facilities where capacity information is available on the website [51], the value is recorded in the capacity column. For facilities where capacity data is unavailable, the estimated capacity is provided in a separate column as estimated capacity.

The first eight shelters listed in Table 1 were open on January 12th. The three shelters at the bottom, along with additional facilities from [51], were included to evaluate how accessibility could be improved by incorporating more potential shelters—one of the key objectives of this study, as outlined in the introduction.

3.2. Population

Initially, we considered using American Community Survey (ACS) population estimates at the census block group (CBG) level, the smallest geographic unit with available population data. However, CBG-based estimates assume uniform population distribution within each polygon, which is problematic in regions like Palisades

Table 1: Shelter locations and capacities during the Palisades and Eaton wildfires

Location	Capacity	Estimated Capacity
Ritchie Valens Recreation Center	356	
Van Nuys/Sherman Oaks Recreation Center		100
Calvary Community Church		797
Pan Pacific Recreation Center	598	
Westwood Recreation Center	855	
Stoner Recreation Center	350	
Pasadena Civic Auditorium		910
Pomona Fairplex		1056
Glendale Civic Center		202
Lanark Recreation Center	100	
El Camino Real Charter High School	1100	

and Eaton, where large portions are forested and sparsely populated. In some areas, CBGs cover vast mountainous regions, leading to inaccurate estimates—for instance, in a certain CBG, 90% of the land is uninhabited, yet the data assumes even distribution across both populated and unpopulated areas. To address this issue, we used LandScan [56], which offers a higher resolution than CBGs and more accurately represents population distribution by avoiding assignments to forests and mountainous areas, as identified through satellite imagery. LandScan provides 1 km resolution grid data, representing a 24-hour average ambient population, estimated using a remote sensing-based global modeling and mapping approach [56]. LandScan also was used in previous accessibility studies [57, 58]. For insights on how population distribution from different datasets, including LandScan, affects spatial accessibility evaluations, see [59]. Figure 2 shows the population distribution in Palisades and Eaton fire evacuation zones and the capacity of eleven shelters listed in Table 1. Land cover (forest or residential) can be examined by switching base layers to OpenStreetMap or satellite imagery in the online map (link in the figure caption).

3.3. Road Network

The road data were collected from OpenStreetMap (OSM) [60], which are a widely used dataset to compute travel cost in previous accessibility studies [61, 58, 35, 34, 33]. We retrieved the OSM road network dataset using the Python package OSMnx [62], which allows for the downloading and analysis of street networks from OpenStreetMap. Given the sparse road networks, particularly in mountainous regions, we included all drivable roads, including service roads such as alleys and parking lot

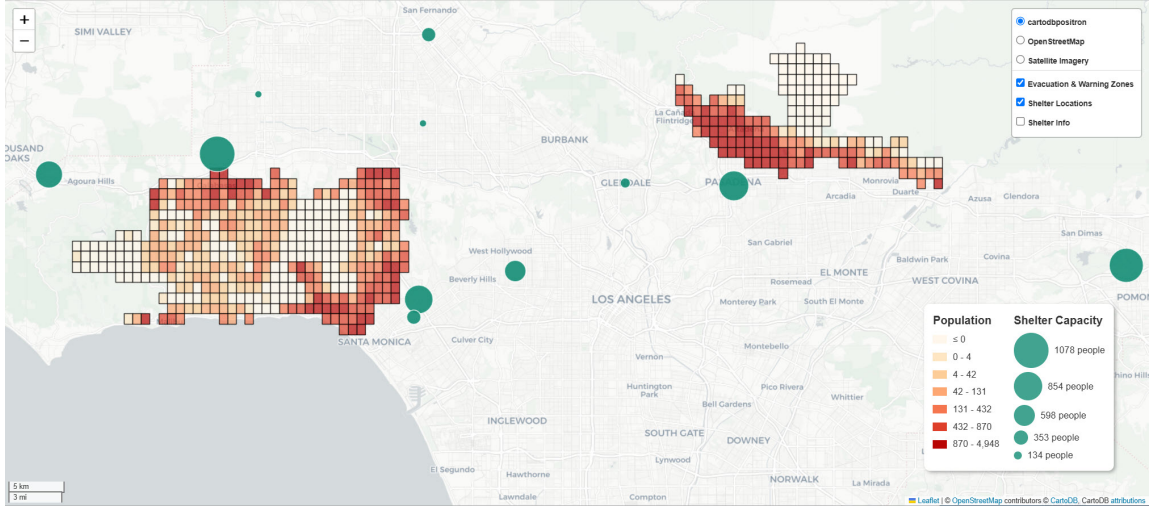


Figure 2: Population distribution based on LandScan Global 2023 data. *Interactive version available at: <https://sites.google.com/view/palisades-and-eton-fires/figure-2>*

roads, to ensure comprehensive coverage. Figure 3 depicts the road network used in our study, which is extensive enough to cover wildfire-related evacuation routes surrounding shelters. The final road network dataset we downloaded contained 701,470 line features.

4. Method

4.1. Accessibility Measurement

We applied the Enhanced Two-Step Floating Catchment Area (E2SFCA) method to assess spatial accessibility between supply locations (i.e., shelters) and demand (i.e., population within each grid cell located in evacuation and warning zones). The E2SFCA method [32] builds upon the original Two-Step Floating Catchment Area (2SFCA) method developed by [37]. It has been widely adopted in numerous studies, particularly for evaluating accessibility to healthcare services [35, 34, 33]. The E2SFCA method calculates accessibility in two steps, considering supply (shelter capacity), demand (population in each grid cell), and the travel cost between supply and demand locations, measured in time or distance. A key feature of this method is its incorporation of distance decay, which assumes that locations closer to a supply point have a greater influence, whereas those farther away have a lesser impact [63]. As the name suggests, the method consists of two steps.

In the first step, for each shelter location j , search all population locations (k) in each grid that are within a threshold travel time (t_0) from location j (this is the

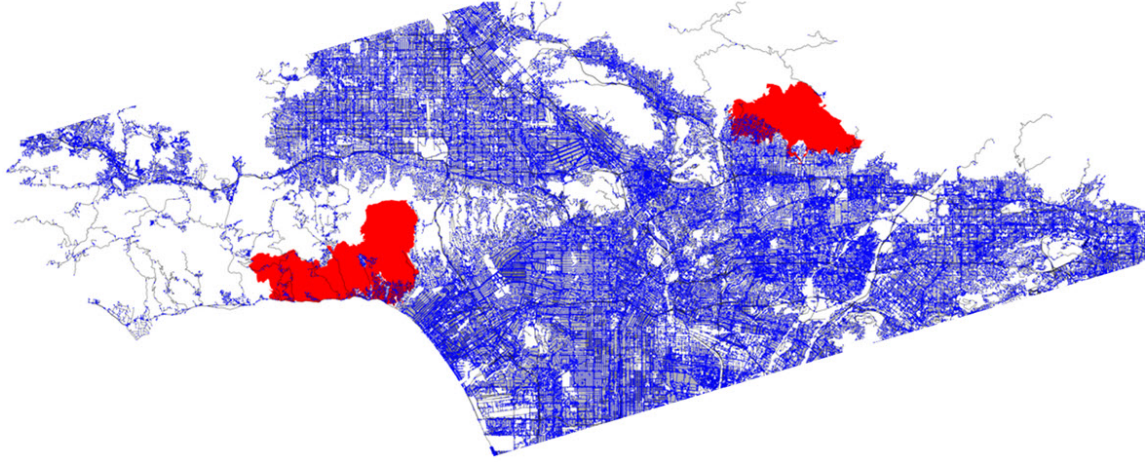


Figure 3: Road network data retrieved from OpenStreetMap (OSM) for our study area.

catchment of shelter location j or catchment j), and compute the weighted shelter-to-population ratio, R_j , within the catchment area as follows:

$$R_j = \frac{S_j}{\sum_{k \in t_{kj} \leq t_0} P_k W_{kj}},$$

where:

- R_j is the supply-to-demand ratio at shelter location j , representing the shelter capacity relative to the population it serves.
- S_j is the degree of supply at shelter location j , measured as the shelter's capacity (e.g., number of evacuees it can accommodate).
- P_k is the degree of demand at location k , measured as the population in grid cell k whose centroid falls within the catchment j (i.e., where $t_{kj} \leq t_0$).
- t_{kj} is the travel time between population grid cell k and shelter location j
- t_0 is the travel time threshold, set to 2 hours in this study.
- W_{kj} is a Gaussian-weighted distance decay function applied to the distance between the population grid cell k and the shelter location j .

In the second step, each population grid i searches for shelter locations j within its catchment area and sums up R_j values of these shelter locations. The equation

for Step 2 is defined as follows:

$$A_i = \sum_{j \in \{t_{ij} \leq t_0\}} R_j W_{ij},$$

where:

- A_i is the accessibility measure at location i .
- R_j is the supply-to-demand (shelter-to-population) ratio at shelter location j which falls within the catchment area centered on population location i (i.e., where $t_{ij} \leq t_0$).
- t_{ij} is the travel time between population grid cell i and shelter location j
- W_{ij} is the same Gaussian distance weights used in Step 1.

The Spatial Access module in PySAL (The Python Spatial Analysis Library) [64] includes an implementation of the Enhanced Two-Step Floating Catchment Area (E2SFCA) method, available through the function `Access.enhanced_two_stage_fca` [65]. One of the input parameters required for this function is the weight function W_{ij} , as defined in the above equations. Users can specify either a step function or a Gaussian weight function with a specified width (σ). In this study, we applied a Gaussian weight function with $\sigma = 30$.

4.2. Computing Travel Cost

Travel time was computed based on the length and maximum speed of road segments within street networks extracted from OpenStreetMap (OSM). As indicated in the equation above, the accessibility score is influenced not only by supply and demand but also by travel cost, which plays a crucial role in shaping access. The OSM street network includes road classification, segment length, and maximum speed, all of which vary based on road type. For instance, motorways, secondary roads, and service roads have maximum speeds of 65 mph, 35 mph, and 15 mph, respectively. When the maximum speed was unavailable for a road segment, we imputed a value based on the mean maximum speed value for edges categorized by highway type, using a function provided by the OSMnx Python package [62]. Using the same package, we also computed travel times by leveraging the maximum speed and segment length for each road or line segment. Additionally, to compute the shortest paths from each demand location to all shelter locations, we employed Dijkstra’s algorithm, a single-source shortest path algorithm, where the weight of an edge in the network

is an estimated travel time from the starting vertex to the ending vertex of the edge. The travel cost, essential for measuring accessibility, was estimated by computing travel times along the shortest path from each demand location (i.e., each grid cell in Figure 2) to each shelter location. In addition, when computing spatial accessibility under traffic congestion [66], a maximum travel speed of 10 kph was assigned to the road network within a five-kilometer buffer zone around the Palisades and Eaton evacuation areas shown in Figure 2. This assumes that vehicles could not travel at the designated road speeds and are instead limited to an average of 10 kph due to severe traffic jams and gridlock [66].

4.3. *Measuring Disparities in Accessibility*

We employ Gini coefficients to measure regional disparities in spatial accessibility to shelters. The Gini coefficient, a classical tool commonly used to measure income inequality, is also widely applied in evaluating the degree of imbalance in access to public service facilities [67, 68, 40, 69, 70, 71, 72, 73]. The Gini coefficient is an effective measure for our study because it helps evaluate how evenly shelter access is distributed. Its values range from 0 to 1, where a lower Gini coefficient indicates more equitable access to shelters, while a value of 1 represents complete inequality. Specifically, a Gini coefficient of 0 reflects a perfectly uniform distribution, whereas a value of 1 indicates full concentration or extreme disparity.

The Gini coefficient is given by [72]:

$$G = 1 - \sum_{i=0}^n (X_{i+1} - X_i)(Y_{i+1} + Y_i),$$

where X_i denotes the cumulative proportion of the population within the population grid used for accessibility calculation, and Y_i represents the cumulative proportion of accessibility to shelters.

4.4. *Workflow of This Study*

To illustrate the methodology employed in this study, Figure 4 shows the complete workflow used in this study to assess shelter accessibility during wildfire events. Inputs and outputs are represented by parallelograms—those labeled with an ‘I’ indicate inputs, while those starting with an ‘O’ represent outputs. Processes are shown as rectangles, each beginning with a ‘P’ to denote a specific procedure or step.

The study’s workflow is organized into four distinct cases, each tailored to evaluate accessibility, as detailed in Table 2, under varying spatial and situational conditions. Specifically, we considered different configurations of shelter (i.e., supply)

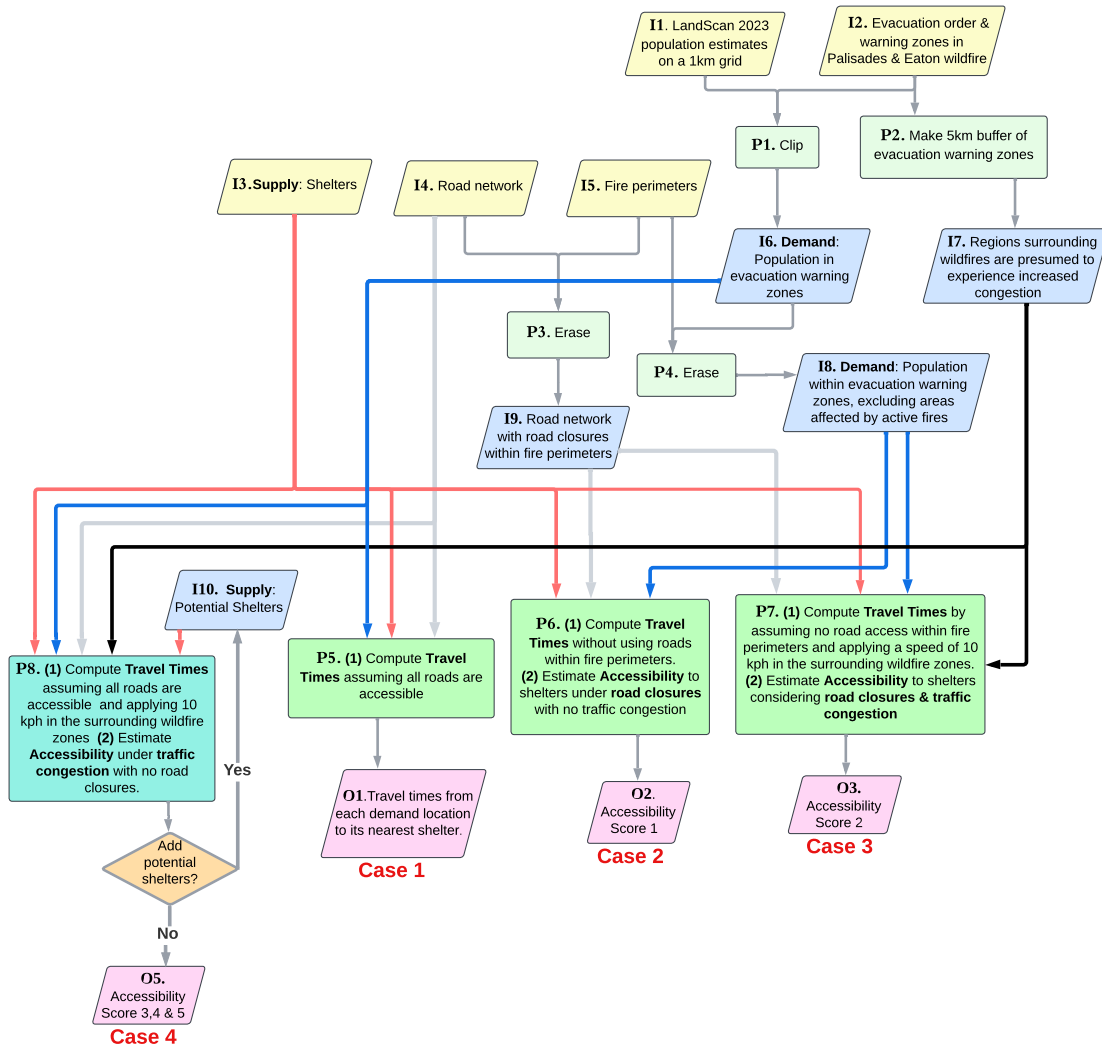


Figure 4: A diagram depicting work flow of this study

availability, including hypothetical shelters; diverse demand areas based on evacuation orders, warning zones, and the presence or absence of active fire areas; and variations in travel cost, accounting for traffic congestion and road closures.

Cases 1 through 3 focus on real-world conditions during the peak wildfire crisis on January 12, while Case 4 examines hypothetical scenarios aimed at enhancing shelter access. On this day, a significant gap existed between available shelter capacity and the number of people living in evacuation zones. The eight operational shelters available on January 12 (the top eight listed in Table 1) had a combined capacity of only 5,224 people. In contrast, population estimates from LandScan Global 2023 indicate that 44,348 individuals were located in evacuation order zones and 42,263 in warning zones, totaling 86,611 people at risk. This left approximately 81,387 people without access to designated shelters. The large gap between available shelter capacity and evacuation demands highlights the immediate need to increase shelter infrastructure to better protect evacuees during such emergencies. The critical gap between available shelter spaces and evacuation requirements on January 12 led to the creation of Case 4, which investigated potential solutions by adding hypothetical shelter sites. Specifically, we examined potential shelter sites drawn from the National Shelter System Facilities dataset ([51]), which includes buildings that could potentially serve as shelters and specify their capacities.

The objective of Case 4 is to identify the locations and capacities of additional shelters needed to accommodate the entire evacuated population and to improve overall accessibility. To achieve this, we designed two sub-scenarios that determine which shelters should be selected and how they should be spatially distributed.

- **Case 4.1: Capacity-based Approach** — The idea of this approach is that when there are too many shelters with small capacities, resources needed for evacuees—such as cots, blankets, food, and medical assistance—must be distributed across multiple locations. By prioritizing larger shelters, the approach aims to minimize logistical efforts and enhance the efficiency of resource allocation during emergencies. Our capacity-based greedy algorithm consists of two steps: filtering and refinement. In the filtering step, starting from the demand areas, the algorithm incrementally searches for the nearest shelters and adds them one by one until their combined capacity exceeds k times the required demand. In our empirical analysis, when $k=2$, shelters within a reasonable distance are included. In the refinement step, the algorithm selects shelters in descending order of capacity from the candidates, starting with the largest, until the total capacity becomes sufficient to accommodate the estimated population in need.

- **Case 4.2: Distance-based Approach** — The intuition behind this approach is to provide evacuees with the nearest possible shelter locations, thereby reducing the time and distance needed to reach shelters. Our distance-based greedy algorithm is described as follows. Starting from the demand areas, the algorithm performs a buffer-based search, incrementally increasing the buffer distance (for example, from 1 mile to 2 miles, and so on). The algorithm continues expanding buffer distances until the total shelter capacity reaches the required demand.

Table 2: Summary of the four case scenarios and procedures used in this study. The labels (e.g., I3, P5) correspond to the input, output and process labels shown in the diagram in Figure 4.

Case	Input: Supply	Input: Demand	Input: Road Network	Traffic Congestion	Process	Output
Case 1	I3. 8 shelters opened on Jan 12th	I6. All population in evacuation order & warning zones	I4. Full road network	Not considered	P5. Compute travel time from each demand location to its nearest shelter	Figure 5: Travel times from each grid cell to its nearest shelter
Case 2	I3. 8 shelters opened on Jan 12th	I8. Population within evacuation order & warning zones, excluding areas affected by active fires	I9. Road network excluding roads within fire perimeters	Not considered	P6. Compute accessibility using specified supply, demand, and road network	Figures 6 & 8: Accessibility with road closures
Case 3	I3. 8 shelters opened on Jan 12th	I8. Population within evacuation order & warning zones, excluding areas affected by active fires	I9. Road network excluding roads within fire perimeters	I7. Considered	P7. Compute accessibility using specified supply, demand, and road network with congestion	Figure 7: Accessibility with road closures and traffic congestion
Case 4	Varied hypothetical shelters	I6. All population in evacuation order & warning zones	I4. Full road network	I7. Considered	P8. Compute accessibility using specified supply, demand, and road network with congestion	Figures 9 & 10: Accessibility based on hypothetical shelters sized for all residents Figure 11: Accessibility to 8 shelters opened on Jan 12th

The demand for shelter accessibility included the population in both evacuation order and warning zones to realistically represent evacuation behaviors observed in recent wildfire events. During wildfire events, the observed evacuation behavior showed that residents from both evacuation order and warning zones chose to evacuate even without official orders, which contradicts the widely held belief that only those in evacuation order zones would evacuate. During the Palisades Fire in January 2025, evacuation started before official orders were given, as people noticed that homes were already burning and traffic congestion had formed by the time they received official evacuation orders [74]. For this reason, many people from evacuation warning zones decided to leave their homes voluntarily during high-risk and fast-changing conditions, similar to residents in evacuation order zones. The unpredictable fire behavior and rapid spread forced residents of both zones to seek shelter before receiving official orders. Therefore, to assess shelter accessibility, we considered the population in both evacuation warning and evacuation order zones as the demand in the spatial accessibility analysis.

5. Results

5.1. *Distance to nearest shelters*

General insights into travel times to shelters can be drawn from Figure 5. In this map, the color shading of each grid cell represents estimated travel times to the nearest shelters under conditions without road congestion. For the Palisades Fire, the southeastern regions within the evacuation order and warning zones generally have shelters located within approximately 3 to 8 minutes, indicating relatively easy access compared to other areas. In contrast, travel times from the inner mountainous regions can extend up to 40 minutes. For the Eaton Fire, the Pasadena Civic Auditorium is the closest shelter for residents in the evacuation order zones. Travel times to this location are generally up to 20 minutes, except for the mountainous areas. In these sparsely populated mountain regions, travel times are more than double those in residential zones. Figure 5 illustrates travel times only to the nearest shelters whose capacities were significantly smaller than the demand as discussed in the section 4.4; as a result, many evacuees had to travel to shelters farther away than the closest ones.

5.2. *Shelter accessibility under congested and uncongested traffic conditions*

Figure 6 presents spatial accessibility scores on January 12—the day the wildfire reached its largest extent, and eight shelters were operational. Roads within the active fire perimeters, marked in red, were considered inaccessible. It was assumed that all populations within these zones had already evacuated, so they were

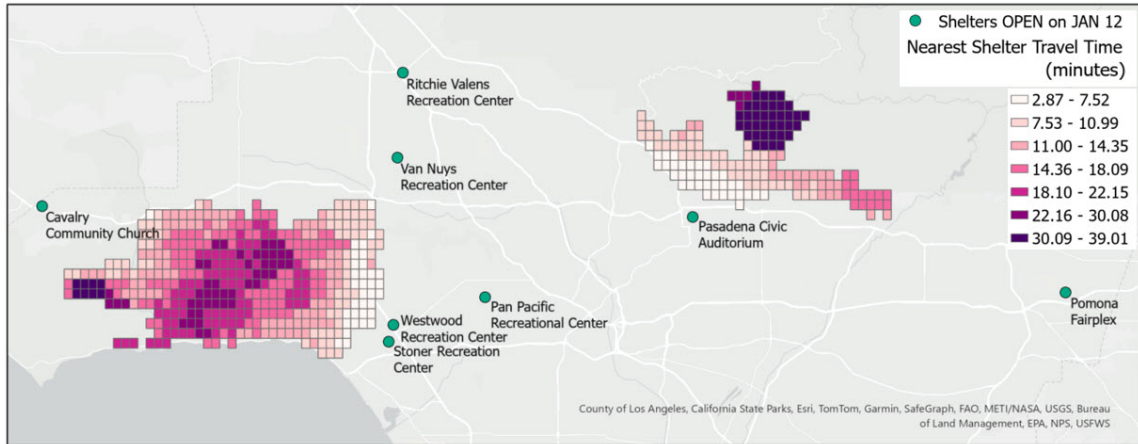


Figure 5: Travel times from each demand location (i.e., each grid cell) to its nearest shelter, based on Case 4 described in Table 2 and illustrated in Figure 4.

excluded from the demand calculations. Shelter capacities were also adjusted to reflect evacuees already accommodated. Accessibility scores on this day ranged from 0 to 2.86. In the Palisades evacuation zones, accessibility was generally higher on the eastern side toward Los Angeles, while lower scores were observed in mountainous areas and the southwestern portion of the zones. In the Eaton evacuation zones, scores ranged from 2.5 to 2.86 in southern residential areas, indicating relatively good access. However, some sparsely populated grids—particularly in the northern mountainous region—showed scores of zero due to road closures that blocked evacuation routes.

Figures 7 and 8 build upon this baseline to examine the impact of traffic congestion on spatial accessibility. Figure 7 reflects congested traffic conditions, as defined in Case 2 of Table 2 and Figure 4, where travel times were significantly increased due to congestion. In this scenario, not only were roads within the fire perimeters closed, but travel within a five-kilometer buffer zone around the evacuation areas was assumed to be extremely limited, with speeds reduced to just 10 kph.

Figure 8 reclassifies the results from Figure 6 using the same interval scheme as Figure 7, allowing for direct comparison between conditions with and without congestion. Both maps use harmonized class intervals—*No Access*, *Very Poor*, *Poor*, *Moderate*, *Good*, *Very Good*, and *Excellent*—to depict differences in accessibility levels across scenarios.

The comparison between Figures 7 and 8 highlights the negative impact of traffic congestion on equitable access to shelters. Figure 8, which depicts accessibility

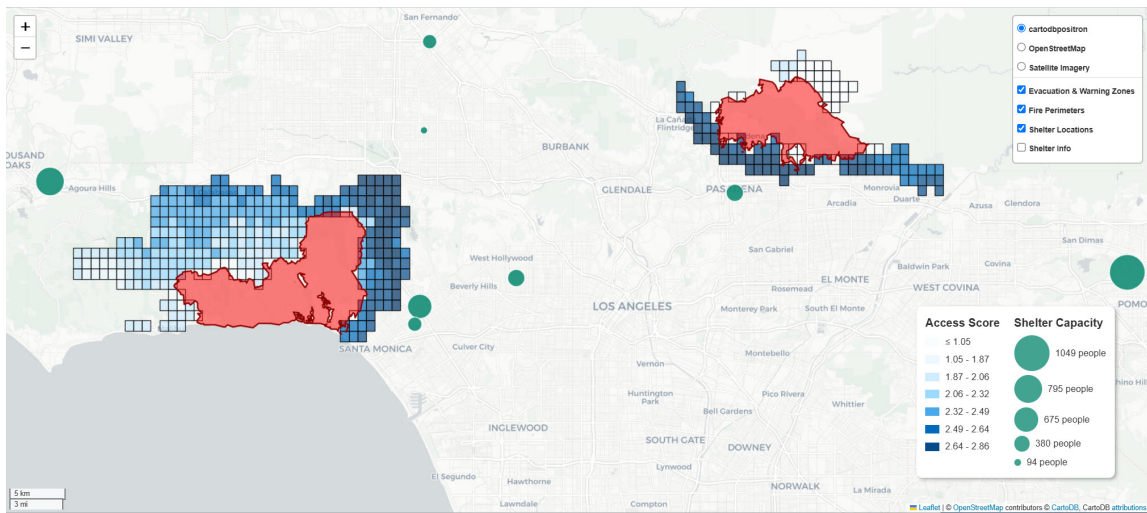


Figure 6: Shelter accessibility from evacuation order and warning zones on January 12, assuming road closures but no traffic congestion. Interactive version available at: <https://sites.google.com/view/palisades-and-eton-fires/figure-6>

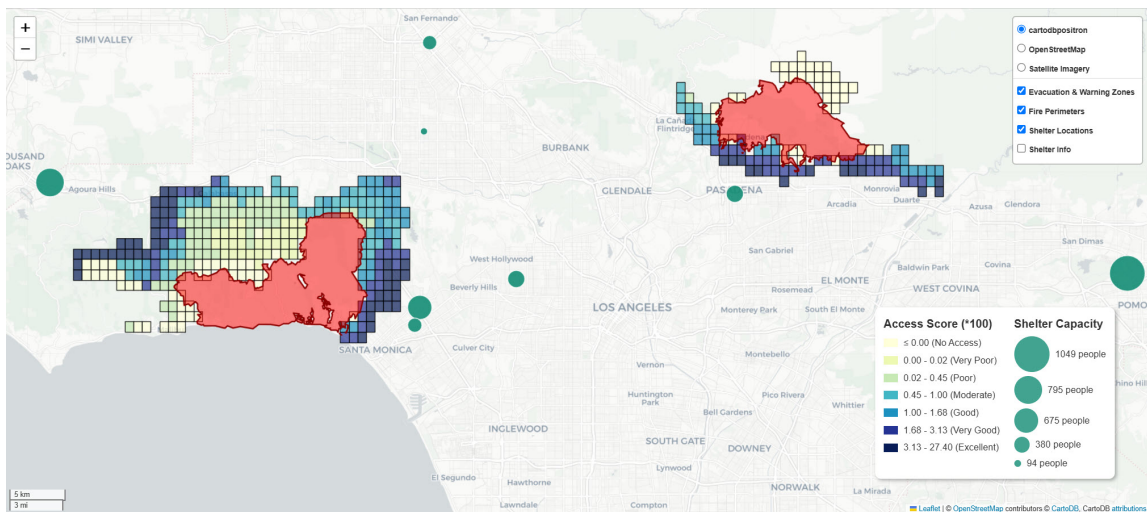


Figure 7: Shelter accessibility from evacuation order and warning zones on January 12, accounting for road closures and traffic congestion. Interactive version available at: <https://sites.google.com/view/palisades-and-eton-fires/figure-7>

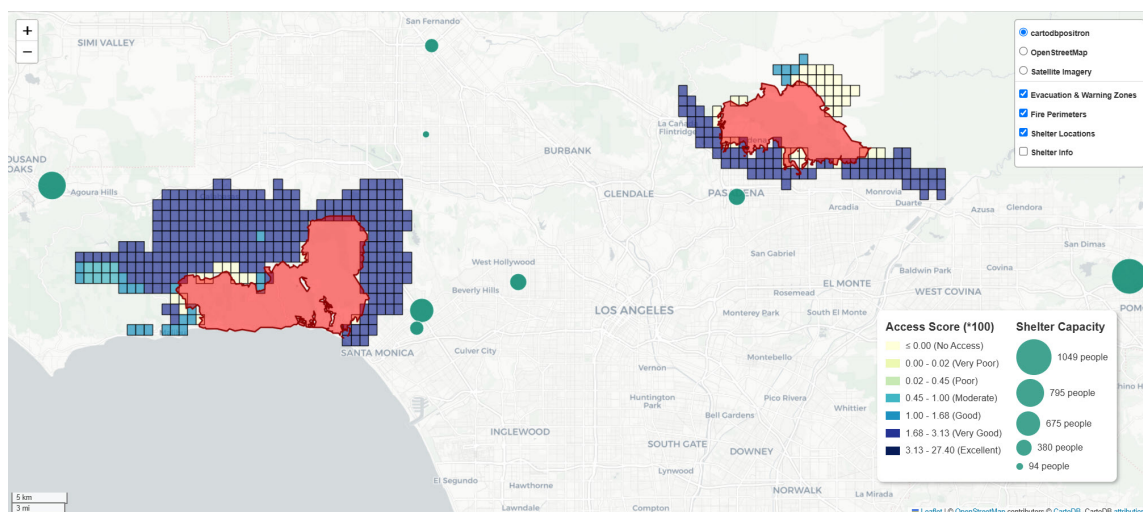


Figure 8: Shelter accessibility from evacuation order and warning zones on January 12, accounting for road closures but without traffic congestion. Interactive version available at: <https://sites.google.com/view/palisades-and-eton-fires/figure-8>

without congestion, shows generally high access across most of the study area—except near active fire perimeters and in regions with sparse road networks, particularly in the southwestern Palisades zones and the mountainous areas of the Eaton evacuation zones. In contrast, Figure 7, which incorporates the effects of traffic congestion, reveals a substantial decline in accessibility. Only a few areas—such as narrow areas the northwest and southeast Palisades fire evacuated zones and a small region near the Pasadena Civic Auditorium near Eaton fire evacuated zones—maintain high accessibility scores. Most other areas fall into the *Very Poor* to *Moderate* accessible categories, indicating a widespread decline in shelter access under congested conditions.

This disparity is further supported by Gini coefficients, which quantify accessibility inequality. The coefficients for Figures 7 and 8 are 0.45 and 0.09, respectively, demonstrating a significant increase in inequality under congested traffic conditions.

5.3. Shelter accessibility with hypothetical shelter locations

As discussed in Section 4.4, approximately 81,387 individuals were left without access to designated shelters. In this section, we explore strategies for the placement of additional shelters to accommodate the entire at-risk population and improve overall accessibility during wildfire emergencies. Specifically, we apply two approaches introduced in Section 4.4—the Capacity-based Approach (Case 4.1) and the Distance-based Approach (Case 4.2). Both cases assume traffic congestion, with travel speeds

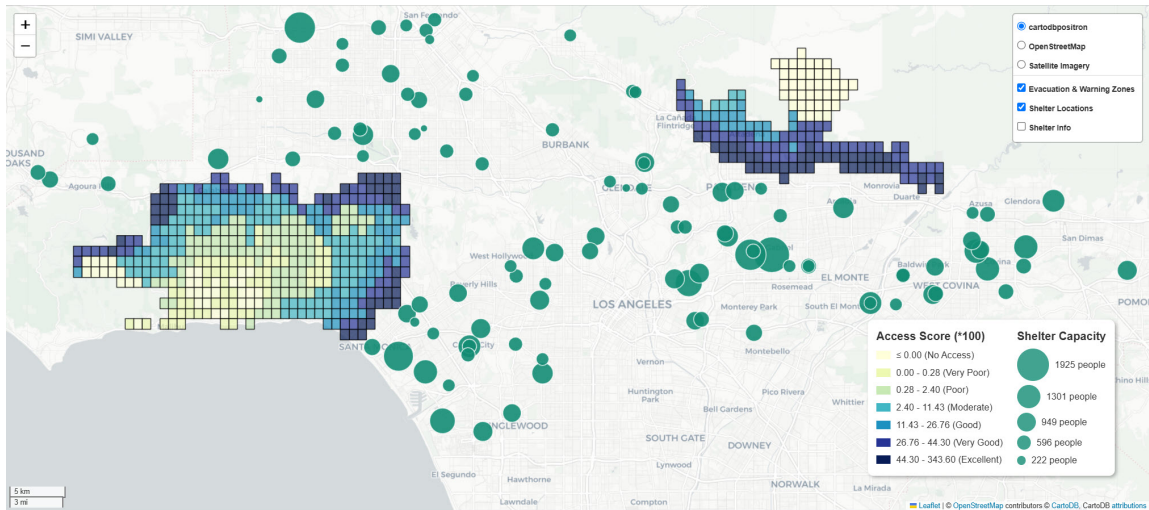


Figure 9: Shelter accessibility based on hypothetical shelters sized to accommodate all residents. A greedy algorithm prioritized shelters with the largest capacities until population needs were met. Interactive version: <https://sites.google.com/view/palisades-and-eton-fires/figure-9>

reduced to 10 kph within a five-kilometer buffer zone surrounding the evacuation areas, consistent with the previous scenario.

Figure 9 presents the results of the Capacity-based Approach, as outlined in Case 4.1 of Section 4.4. In this scenario, the first eleven shelters used during the Palisades and Eaton wildfires were included, providing a combined capacity for 6,424 evacuees—significantly below the total at-risk population of 86,661 within the evacuation zones. To address this shortfall, the algorithm began from demand areas (i.e., the Palisades and Eaton zones) and incrementally searched for additional potential shelters drawn from the National Shelter System Facilities dataset ([51]) by expanding buffer distances outward. Shelters were added one by one until the combined capacity reached twice the estimated demand (173,222 people) to ensure sufficient coverage. This threshold was reached at approximately 13 kilometers from the evacuation zones. At that point, shelter selection was finalized by choosing facilities within the 13-kilometer buffer in descending order of capacity—starting with the largest—until the cumulative shelter capacity met or exceeded the population in need (86,661 people). Through this process, the selected shelters shown in Figure 9 were identified, offering a total combined capacity of 86,957 evacuees.

Figure 10 presents the results of the Distance-based Approach (Case 4.2). Similar to the Capacity-based Approach, this method began by including the eleven existing shelters, which together provided a total capacity of 6,424 evacuees. However, un-

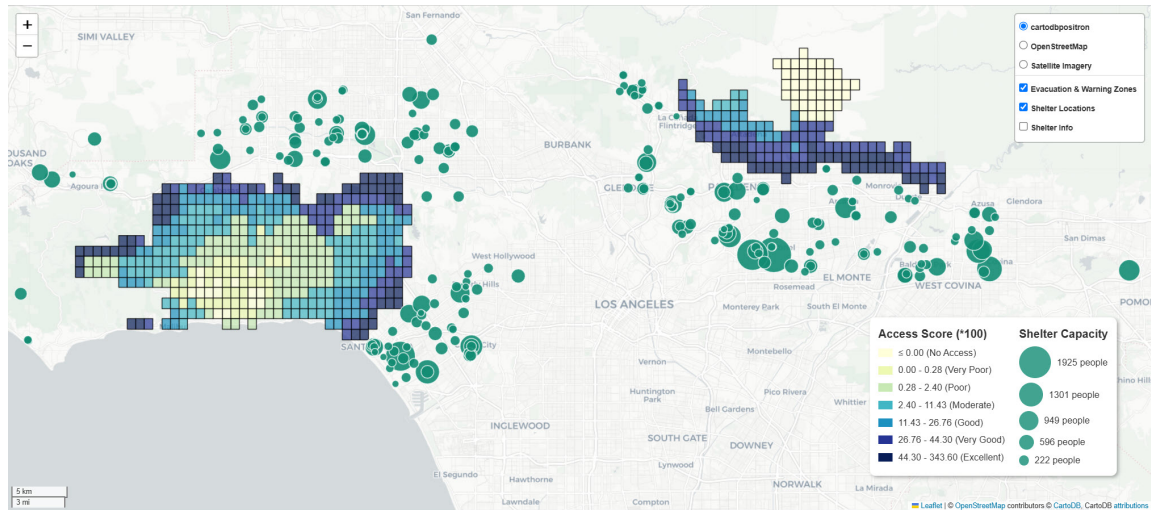


Figure 10: Shelter accessibility based on hypothetical shelters sized to accommodate all residents. Shelters were incrementally added in order of proximity until the entire population in evacuation and warning zones was covered. Interactive version: <https://sites.google.com/view/palisades-and-eaton-fires/figure-10>

like the Capacity-based Approach, to accommodate the remaining population—40,092 individuals in the Palisades evacuation zones and 40,095 in the Eaton zones—a buffer-based search was conducted outward from each demand area. The algorithm incrementally expanded the buffer distance, adding the nearest available shelters until the cumulative shelter capacity, based on the National Shelter System Facilities dataset [51], met or slightly exceeded the required demand for each zone. The selection process concluded once the total shelter capacity reached 40,157 for the Palisades zone and 41,374 for the Eaton zone.

The resulting distribution of shelters is shown in Figure 10. Unlike the shelter pattern in Figure 9, which focuses on maximizing total capacity regardless of location, the Distance-based Approach in Figure 10 yields a more spatially clustered distribution, with shelters located closer to the evacuation zones. This outcome reflects the algorithm’s emphasis on minimizing travel distance for evacuees by prioritizing proximity over shelter capacity.

Shelter placements using the Capacity-based Approach (Figure 9) and the Distance-based Approach (Figure 10) show greater improvements in accessibility compared to the actual eleven shelters opened on January 12, as shown in Figure 11. Figure 11 presents the accessibility scores under the same traffic congestion scenario depicted in Figures 9 and 10. To ensure a fair comparison, the color scheme and class intervals

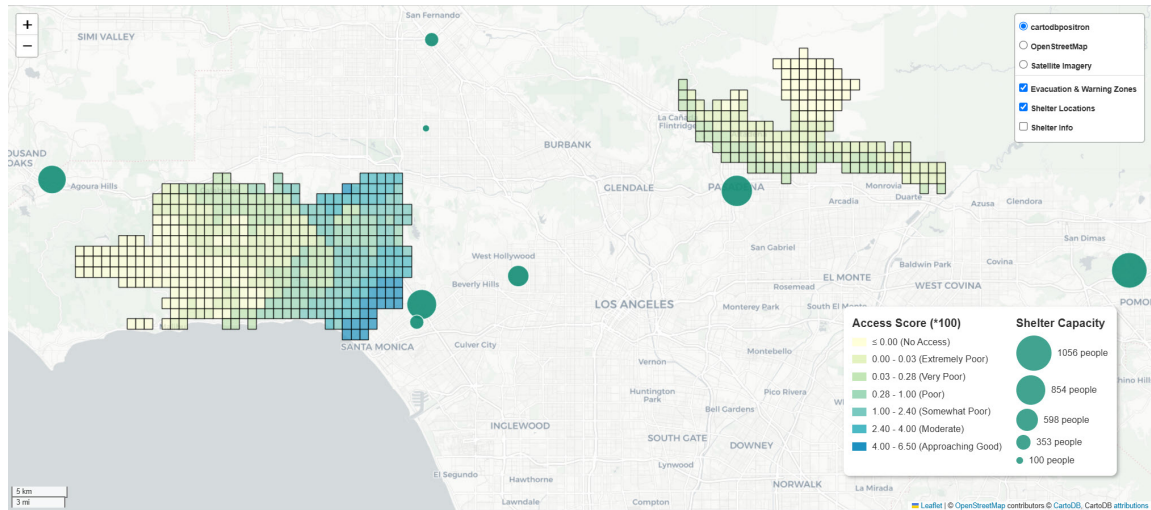


Figure 11: Shelter accessibility from evacuation order and warning zones on January 12, assuming full road network availability and traffic congestion. Interactive version: <https://sites.google.com/view/palisades-and-eton-fires/figure-11>

in Figure 11 were aligned with those in Figures 9 and 10. As expected, the overall accessibility scores in the hypothetical shelter scenarios (Figures 9 and 10) are generally higher across the study area due to the increased number of shelters, compared to the case of eleven shelters in Figure 11. When examining equity in shelter access across the three scenarios, the Gini coefficient is 0.34 for the Capacity-based Approach and 0.31 for the Distance-based Approach (Figure 10), while the original 11-shelter scenario (Figure 11) shows a much higher Gini coefficient of 0.69. This indicates significantly greater disparities in shelter access under the actual 11-shelter scenario.

Between the two hypothetical strategies in Figure 9 and 10, the Distance-based Approach shows slightly better equity, as indicated by its lower Gini coefficient. This suggests that the Distance-based approach provides more equal access to shelters than the Capacity-based Approach. The likely reason is that it prioritizes the minimum travel distance and time for evacuees, while the Capacity-based Algorithm focuses on reducing the number of shelters required, emphasizing efficiency and logistical resource distribution.

6. Conclusion

This research investigates four essential research questions focused on how accessible shelters were during the 2025 wildfires in Palisades and Eaton. First, the

analysis showed that during the wildfire peak period shelter accessibility was inadequate because eight shelters with a total capacity of 5,224 served more than 86,000 evacuees, leaving the vast majority without access to formal shelter access. Second, evacuees needed to travel significantly varying length of time to reach the nearest shelters which often took more than 30–40 minutes from mountainous and remote areas during normal conditions but became even longer due to road closures and traffic congestion. Third, there were notable geographic disparities in shelter accessibility, particularly in isolated areas lacking sufficient road infrastructure. Lastly, the implementation of strategic shelter placement using the Capacity-based and Distance-based Approaches demonstrated substantial improvements in both shelter accessibility and equity in access by expanding shelter capacity and efficient allocation of shelter locations which provided actionable future emergency solutions.

The results from our study provide multiple policy implications for improving disaster preparedness and resilience in areas that frequently experience wildfires.

First, shelter placement is crucial in improving accessibility during wildfire evacuations. Our analysis demonstrates that accessibility can be significantly improved through strategic shelter placement. Utilizing the Capacity-based and Distance-based approaches, we proposed shelter placements to enhance access and bolster urban resilience in emergency situations. Our results suggest that data-driven planning approaches can enhance readiness and resilience against disasters in wildfire-prone regions. To achieve this, emergency management agencies need to develop region-specific plans that align shelter availability with projected displacement figures, using detailed population data. Additionally, state and county authorities should establish minimum shelter-to-population standards for high-risk regions to maintain sufficient emergency service capacity and equitable distribution of emergency resources.

Second, enhancing urban resilience to wildfires necessitates forward-thinking planning and strategic investment in shelter facilities. Proactive site designation and infrastructure investment are essential for achieving emergency readiness. Maintaining an up-to-date inventory of potential emergency shelter locations—such as schools and community centers—is essential for rapid deployment during crises. Vulnerable communities and geographically isolated areas need immediate infrastructure enhancements that promote equitable access to emergency shelters. These upgrades should prioritize compliance with the American with Disabilities Act (ADA), along with improvements to sanitation and ventilation systems. Equally important is the inclusion of spatial equity in emergency planning. Shelter siting should consider geographic distribution, road network limitations, and vulnerable population so that all communities—not just those in urban centers—have fair access to life-saving services. It should also be noted that collaboration between transportation agencies and

emergency managers is vital to enhance urban resilience planning for disaster events. Integrating real-time traffic updates and evacuation simulations into preparedness plans will help reduce congestion and prevent access bottlenecks during evacuations.

Finally, key elements to building resilient communities include scenario-based preparedness drills together with forward-looking policies. Local authorities should routinely conduct exercises to test shelter accessibility under various hazard scenarios, using simulations like those developed in this study. Through routine preparedness drills, local planners and decision-makers can move from reactive approaches—where they respond only after a disaster happens—to proactive systems that are based on data-driven systems designed to ensure fair access to shelters for everyone. Given the increasing frequency and intensity of climate-driven disasters coupled with growing unpredictability, it is essential to view shelter accessibility not only as a logistical necessity but also as a matter of environmental justice. This research offers a framework to guide such efforts and support the development of adaptive and resilient communities.

One limitation of this study is the lack of access to actual traffic congestion data during the the Palisades and Eaton Fires. Without available open-source platforms to provide historical traffic information, we created a theoretical congestion model assuming vehicles moved at 10 kilometers per hour. While some commercial platforms offer historical traffic data, they require purchase and verification of data accuracy, which can be resource-intensive. Incorporating such data in future research could enhance the accuracy of accessibility measurements by reflecting actual travel conditions during the fire events.

This research assessed spatial accessibility on January 12, which marked the peak of wildfire activity. To gain a more comprehensive understanding of evacuation dynamics, future investigations should benefit from analyzing accessibility patterns throughout the entire duration of the wildfire incidents. This includes examining the initial days when fire activity was minimal, as well as the period following January 12 when containment efforts started working out. Additionally, future studies could explore shelter accessibility for vulnerable groups, such as older people and families without access to private vehicles, people under poverty level, communities with low household income, residential areas with low property values, and settlements in harsh environments to better inform equitable evacuation planning.

Appendix A. Shelter Estimation

- Shelter location: Van Nuys/Sherman Oaks Recreation Center

Estimating the shelter capacity for the Van Nuys/Sherman Oaks Recreation

Center at 14201 Huston St., Sherman Oaks, CA, involves assessing the available indoor space. The recreation center features a 15,000-square-foot gymnasium, which serves as a significant indoor space suitable for sheltering purposes [52]. Standard estimates suggest that about 30% of the total indoor space is unusable due to hallways, storage areas, restrooms, and other non-shelterable spaces. With a total indoor space of 15,000 square feet, the estimated usable space is 10,500 square feet, calculated as $15,000 \text{ sq. ft.} \times 0.70$. Based on an assumption that each person requires 100 square feet, the estimated shelter capacity for the facility is approximately 105 people.

- Shelter location: Calvary Community Church at 5495 Via Rocas, Westlake Village, CA

The building area measured from the satellite image is $10,573.27 \text{ m}^2$. After excluding 30% for unusable space, the estimated shelter capacity for Calvary Community Church is approximately 797 people, assuming that each person requires 100 sq. ft.

- Shelter location: Pasadena Civic Auditorium

Estimating the shelter capacity of the Pasadena Convention Center at 300 E Green Street, Pasadena, CA, involves determining the usable indoor area. The convention center offers approximately 130,000 square feet of flexible event space, including exhibit halls, ballrooms, and meeting rooms [75]. Without detailed floor plans, it is standard to estimate that about 30% of the total space is unusable due to hallways, storage areas, restrooms, and other non-shelterable areas. Given a total building area of 130,000 square feet, the estimated unusable space is 39,000 square feet, resulting in a usable area of approximately 91,000 square feet. Assuming that each person requires 100 square feet, the estimated shelter capacity for the facility is approximately 105 people.

- Shelter location: Pomona Fairplex

The Fairplex offers approximately 325,000 square feet of indoor exhibit space, with several major exhibition halls that can be utilized for sheltering purposes [76]. Building 4, the largest of these spaces, covers approximately 105,600 square feet with a length of 770 feet and a width ranging from 130 to 146 feet. It also features a stage measuring 64 by 19 feet and includes eight dressing rooms. Buildings 5, 6, 7, and 8 each provide 33,600 square feet, with dimensions of 100 feet by 318 feet. Each of these buildings is equipped with its own ticket office and two 360-square-foot show support offices. Building 3, covering

approximately 11,486 square feet, is divided into five interior rooms, offering flexibility for various uses. These facilities are designed to accommodate a wide range of events, from large-scale exhibitions to more intimate gatherings [76]. The total indoor area of the major exhibition halls, including Building 4 (105,600 sq. ft.), Buildings 5–8 (33,600 sq. ft. each), and Building 3 (11,486 sq. ft.), sums to approximately 150,686 square feet. After excluding 30% for unusable space, the estimated shelter capacity for the facility is 1,056 people, assuming that each person requires 100 square feet.

- Shelter location: Glendale Civic Center

Estimating the shelter capacity for the Glendale Civic Center at 613 E Broadway, Glendale, CA 91206, involves assessing the available indoor areas and applying FEMA and Red Cross Emergency Shelter Standards. The Glendale Civic Center provides a variety of spaces suitable for sheltering purposes, with a total meeting space of approximately 28,985 square feet [77]. Considering that 30% of the space is typically unusable due to hallways, storage, and other non-shelterable areas, the estimated usable space is approximately 20,290 square feet. Based on the assumption that each person requires 100 square feet, the estimated shelter capacity for the facility is 202 people .

References

- [1] T. J. Cova, D. M. Theobald, J. B. Norman, L. K. Siebeneck, Mapping wildfire evacuation vulnerability in the western us: the limits of infrastructure, *GeoJournal* 78 (2013) 273–285.
- [2] NASA, Six trends to know about fire season in the western us, accessed: 2025-02-16 (n.d.).
URL <https://science.nasa.gov/earth/natural-disasters/wildfires/six-trends-to-know-about-fire-season-in-the-western-us/>
- [3] NOAA, The wildfire-climate connection, accessed: 2025-02-16 (n.d.).
URL <https://www.noaa.gov/noaa-wildfire/wildfire-climate-connection>
- [4] A. P. Williams, J. T. Abatzoglou, A. Gershunov, J. Guzman-Morales, D. A. Bishop, J. K. Balch, D. P. Lettenmaier, Observed impacts of anthropogenic climate change on wildfire in california, *Earth’s Future* 7 (8) (2019) 892–910.

- [5] Statista, Number of deaths due to wildfires in the united states, accessed: 2025-02-16 (n.d.).
URL <https://www.statista.com/statistics/1422130/usa-number-of-deaths-due-to-wildfires/>
- [6] NBC News, California wildfires: What we know about the victims killed, accessed: 2025-02-16 (n.d.).
URL <https://www.nbcnews.com/news/us-news/california-wildfires-what-we-know-victims-killed-rcna188240>
- [7] Joint Economic Committee Democrats, Climate-exacerbated wildfires cost the u.s. between \$394 to \$893 billion each year in economic costs and damages, accessed: 2025-02-16 (2023).
URL <https://www.jec.senate.gov/public/index.cfm/democrats/2023/10/climate-exacerbated-wildfires-cost-the-u-s-between-394-to-893-billion-each-year-in-economic-costs-and-damages>
- [8] D. Wang, D. Guan, S. Zhu, M. M. Kinnon, G. Geng, Q. Zhang, H. Zheng, T. Lei, S. Shao, P. Gong, et al., Economic footprint of california wildfires in 2018, *Nature Sustainability* 4 (3) (2021) 252–260.
- [9] California Department of Forestry and Fire Protection (CAL FIRE), Palisades fire, accessed: 2025-02-16 (2025).
URL <https://www.fire.ca.gov/incidents/2025/1/7/palisades-fire>
- [10] New York Post, Palisades and eaton fires both 100% contained, california authorities say (2025).
URL <https://nypost.com/2025/02/01/us-news/palisades-and-eaton-fires-both-100-contained-california-authorities/>
- [11] NBC News, Palisades eaton fire in l.a. contained, accessed: 2025-02-16 (n.d.).
URL <https://www.nbcnews.com/weather/wildfires/palisades-eaton-fire-la-contained-rcna188338>
- [12] Los Angeles County Recovery, Media update: Eaton and palisades fires - january 22, 2025, accessed: 2025-02-16 (January 2025).
URL <https://recovery.lacounty.gov/2025/01/22/media-update-eaton-and-palisades-fires-1-22-25/>
- [13] J. Jimenez, J. Healy, L.a. wildfire evacuees scramble to find sleep in shelters, hotels and even cars, *The New York Times* Accessed: 2025-01-30 (January 2025).

URL <https://www.nytimes.com/2025/01/13/us/la-fires-evacuations-housing-shelter.html>

- [14] The New York Times, La fires force evacuations, highlighting housing and shelter crisis, accessed: 2025-02-16 (2025).
URL <https://www.nytimes.com/2025/01/13/us/la-fires-evacuations-housing-shelter.html>
- [15] The New York Times, California fire prompts evacuations in pacific palisades, The New York Times Accessed: 2025-02-16 (January 2025).
URL <https://www.nytimes.com/2025/01/08/us/california-fire-palisades-evacuation.html>
- [16] BBC Future, Why los angeles was so hard to evacuate during the wildfires, accessed: 2025-02-16 (January 2025).
URL <https://www.bbc.com/future/article/20250109-why-los-angeles-was-so-hard-to-evacuate-during-the-wildfires>
- [17] Associated Press, California wildfires and evacuation alerts, accessed: 2025-02-16 (February 2025).
URL <https://apnews.com/article/california-wildfires-evacuation-alerts-69f10d320df14c6394fc2c646d1ff0ce>
- [18] The Guardian, Los angeles' palisades and eaton fires fully contained, officials confirm (2025).
URL <https://www.theguardian.com/us-news/2025/feb/01/los-angeles-palisades-eaton-fires-contained>
- [19] T. J. Cova, F. A. Drews, L. K. Siebeneck, A. Musters, Protective actions in wildfires: evacuate or shelter-in-place?, *Natural Hazards Review* 10 (4) (2009) 151–162.
- [20] T. C. for Emergency Preparedness, Wildfire response and evacuation, accessed: February 18, 2025 (2025).
URL <https://tcep.org/wildfire-response-evacuation>
- [21] T. J. Cova, P. E. Dennison, F. A. Drews, Modeling evacuate versus shelter-in-place decisions in wildfires, *Sustainability* 3 (10) (2011) 1662–1687.
- [22] F. N. Shurtz, Wildfire risk and hillside evacuation strategies, accessed: 2025-02-19 (2025).

URL <https://www.cortemadera.gov/DocumentCenter/View/3795/Wildfire-Risk-And-Hillside-Evacuation-Strategies-from-Chief-Shurtz>

- [23] J. Handmer, A. Tibbits, Is staying at home the safest option during bushfires? historical evidence for an australian approach, *Global Environmental Change Part B: Environmental Hazards* 6 (2) (2005) 81–91.
- [24] G. Baxter, M. Alexander, G. Dakin, Travel rates by alberta wildland firefighters using escape routes on a moderately steep slope. (2004).
- [25] SafeHome.org, Wildfire safety guide, accessed: 2025-02-19 (2025).
URL <https://www.safehome.org/resources/wildfire-safety-guide/>
- [26] A. Ermagun, F. Janatabadi, Compound risk of wildfire and inaccessible shelters is disproportionately impacting disadvantaged communities, *Progress in Disaster Science* 23 (2024) 100358.
- [27] J. Yang, O. Alisan, M. Ma, E. E. Ozguven, W. Huang, L. Vijayan, Spatial accessibility analysis of emergency shelters with a consideration of sea level rise in northwest florida, *Sustainability* 15 (13) (2023) 10263.
- [28] C. Marolla, California wildfires: A holistic systemic management approach to urban resilience (2025). doi:doi:10.33774/coe-2025-ttng2.
- [29] A. W. Dye, J. B. Kim, A. McEvoy, F. Fang, K. L. Riley, Evaluating rural pacific northwest towns for wildfire evacuation vulnerability, *Natural Hazards* 107 (1) (2021) 911–935.
- [30] S. N. Zehra, S. D. Wong, Systematic review and research gaps on wildfire evacuations: infrastructure, transportation modes, networks, and planning, *Transportation Planning and Technology* (2024) 1–35.
- [31] A. M. Fraser, M. V. Chester, B. S. Underwood, Wildfire risk, post-fire debris flows, and transportation infrastructure vulnerability, *Sustainable and Resilient Infrastructure* 7 (3) (2022) 188–200.
- [32] W. Luo, Y. Qi, An enhanced two-step floating catchment area (e2sfca) method for measuring spatial accessibility to primary care physicians, *Health & place* 15 (4) (2009) 1100–1107.
- [33] J. Park, A. Michels, F. Lyu, S. Y. Han, S. Wang, Daily changes in spatial accessibility to icu beds and their relationship with the case-fatality ratio of covid-19 in the state of texas, usa, *Applied Geography* 154 (2023) 102929.

- [34] J.-Y. Kang, A. Michels, F. Lyu, S. Wang, N. Agbodo, V. L. Freeman, S. Wang, Rapidly measuring spatial accessibility of covid-19 healthcare resources: a case study of illinois, usa, *International journal of health geographics* 19 (2020) 1–17.
- [35] J.-Y. Kang, B. F. Farkhad, M.-p. S. Chan, A. Michels, D. Albarracin, S. Wang, Spatial accessibility to hiv testing, treatment, and prevention services in illinois and chicago, usa, *PLoS One* 17 (7) (2022) e0270404.
- [36] M. F. Guagliardo, Spatial accessibility of primary care: concepts, methods and challenges, *International journal of health geographics* 3 (2004) 1–13.
- [37] W. Luo, F. Wang, Measures of spatial accessibility to health care in a gis environment: synthesis and a case study in the chicago region, *Environment and planning B: planning and design* 30 (6) (2003) 865–884.
- [38] J.-Y. Kang, J. Jung, K. Kim, Covid-19 vaccine rollout plans should consider spatial distribution of age-specific population, *The Professional Geographer* 75 (6) (2023) 1034–1044.
- [39] X. Zhu, Z. Tong, X. Liu, X. Li, P. Lin, T. Wang, An improved two-step floating catchment area method for evaluating spatial accessibility to urban emergency shelters, *Sustainability* 10 (7) (2018) 2180.
- [40] H. Su, W. Chen, M. Cheng, Using the variable two-step floating catchment area method to measure the potential spatial accessibility of urban emergency shelters, *GeoJournal* (2021) 1–15.
- [41] Z. Zhang, Y. Hu, W. Lu, W. Cao, X. Gao, Spatial accessibility analysis and location optimization of emergency shelters in deyang, *Geomatics, Natural Hazards and Risk* 14 (1) (2023) 2213809.
- [42] Y. Liang, Z. Xie, S. Chen, Y. Xu, Z. Xin, S. Yang, H. Jian, Q. Wang, Spatial accessibility of urban emergency shelters based on ga2sfca and its improved method: A case study of kunming, china, *Journal of Urban Planning and Development* 149 (2) (2023) 05023013.
- [43] Z. Ding, H. Dong, L. Yang, N. Xue, L. He, X. Yao, A study on the emergency shelter spatial accessibility based on the adaptive catchment size 2sfca method, *ISPRS International Journal of Geo-Information* 11 (12) (2022) 593.

- [44] Y. Xu, C. Zhou, B. Hu, Measuring the accessibility of emergency shelters based on an improved two-step floating catchment area model, *International Journal of Digital Earth* 18 (1) (2025) 2479864.
- [45] L. Zhao, H. Li, Y. Sun, R. Huang, Q. Hu, J. Wang, F. Gao, Planning emergency shelters for urban disaster resilience: An integrated location-allocation modeling approach, *Sustainability* 9 (11) (2017) 2098.
- [46] M. Unal, C. Uslu, Gis-based accessibility analysis of urban emergency shelters: The case of adana city, *The International Archives of the Photogrammetry, Remote Sensing and Spatial Information Sciences* 42 (2016) 95–101.
- [47] A. Mandalapu, K. Seong, J. Jiao, Evaluating urban fire vulnerability and accessibility to fire stations and hospitals in austin, texas, *PLOS Climate* 3 (7) (2024) e0000448.
- [48] K. Kiran, J. Corcoran, P. Chhetri, Measuring the spatial accessibility to fire stations using enhanced floating catchment method, *Socio-Economic Planning Sciences* 69 (2020) 100673.
- [49] California Department of Forestry and Fire Protection, Top 20 destructive ca wildfires, <https://web.archive.org/web/20250124121546/https://34c031f8-c9fd-4018-8c5a-4159cdff6b0d-cdn-endpoint.azureedge.net/-/media/calfire-website/our-impact/fire-statistics/top-20-destructive-ca-wildfires.pdf?hash=97ECEED23181B02019118DB38B63ABBC&rev=582019785a994dccb61e8f554f4d3c2b>, archived via the Wayback Machine on 2025-01-24 (n.d.).
- [50] California Governor’s Office of Emergency Services, Shelters available for communities impacted by wildfires in southern california, accessed: 2025-02-23 (jan 2025).
URL <https://news.caloes.ca.gov/shelters-available-for-communities-impacted-by-wildfires-in-southern-california-4/>
- [51] HIFLD, National shelter system facilities, <https://hifld-geoplatform.hub.arcgis.com/datasets/geoplatform:national-shelter-system-facilities/explore?location=34.072077%2C-118.582547%2C12.40>, accessed: 2025-02-24.
- [52] P. M. Architects, Paul murdoch architects, <https://www.paulmurdocharchitects.com/sherman-oaks-gymnasium>, accessed: 2025-02-22 (n.d.).

- [53] F. E. M. Agency, Fema p-785: Mass care/emergency assistance shelter guidance, Tech. rep., Federal Emergency Management Agency, available at: https://www.nationalmasscarestrategy.org/wp-content/uploads/2015/10/Shelter-Field-Guide-508_f3.pdf (2015).
- [54] S. Project, The Sphere Handbook: Humanitarian Charter and Minimum Standards in Humanitarian Response, 4th Edition, Sphere Association, 2018.
URL <https://spherestandards.org/handbook/>
- [55] Centers for Disease Control and Prevention, Shelter assessment instructions for covid-19, accessed: February 23, 2025 (2020).
URL https://www.cdc.gov/environmental-health-response-and-recovery/media/pdfs/Shelter_Assessment_instructions_COVID508.pdf
- [56] Oak Ridge National Laboratory, Landsat: High-resolution global population data, accessed: 2025-02-24 (2025).
URL <https://landsat.ornl.gov/about>
- [57] J. Cai, C. Huang, Z. Deng, L. Li, Transport accessibility and poverty alleviation in guizhou province of china: Spatiotemporal pattern and impact analysis, *Sustainability* 15 (4) (2023) 3143.
- [58] M. Luqman, S. U. Khan, Geospatial application to assess the accessibility to the health facilities in egypt, *The Egyptian Journal of Remote Sensing and Space Science* 24 (3) (2021) 699–705.
- [59] J. Tan, X. Wang, J. Pan, et al., The effect of population distribution measures on evaluating spatial accessibility of primary health-care institutions: A case study from china, *Geospatial Health* 16 (1) (2021).
- [60] M. Haklay, P. Weber, Openstreetmap: User-generated street maps, *IEEE Pervasive computing* 7 (4) (2008) 12–18.
- [61] S. Liu, C. Higgs, J. Arundel, G. Boeing, N. Cerdera, D. Moctezuma, E. Cerin, D. Adlakha, M. Lowe, B. Giles-Corti, A generalized framework for measuring pedestrian accessibility around the world using open data, *Geographical Analysis* 54 (3) (2022) 559–582.
- [62] G. Boeing, Osmnx: New methods for acquiring, constructing, analyzing, and visualizing complex street networks, *Computers, environment and urban systems* 65 (2017) 126–139.

- [63] J. Park, D. Goldberg, A review of recent spatial accessibility studies that benefitted from advanced geospatial information: multimodal transportation and spatiotemporal disaggregation, *ISPRS International Journal of Geo-Information* 10 (8) (2021) 532.
- [64] PySAL Development Team, Access: Spatial accessibility library, <https://pysal.org/access/>, accessed: 2025-04-30 (2024).
- [65] PySAL Development Team, Access: `enhanced_two_stage_fca` function documentation, https://pysal.org/access/generated/access.Access.enhanced_two_stage_fca.html#access.Access.enhanced_two_stage_fca, accessed: 2025-04-30 (2024).
- [66] Los Angeles Times, Palisades residents face traffic gridlock, panic as fire blazes through community: ‘it looks grim’, accessed: 2025-04-23 (January 2025). URL <https://www.latimes.com/california/story/2025-01-07/pacific-palisades-residents-face-traffic-gridlock-uncertainty-as-the-y-flee-fire-it-looks-grim>
- [67] M. Harada, M. Okayama, R. Ae, T. Kojo, M. Aihara, E. Kajii, A study on regional disparities in access to inpatient care, using the gini coefficient, *General Medicine* 13 (1) (2012) 25–29.
- [68] T. Nakamura, A. Nakamura, K. Mukuda, M. Harada, K. Kotani, Potential accessibility scores for hospital care in a province of japan: Gis-based ecological study of the two-step floating catchment area method and the number of neighborhood hospitals, *BMC health services research* 17 (2017) 1–7.
- [69] H. Wang, X. Wei, W. Ao, Assessing park accessibility based on a dynamic huff two-step floating catchment area method and map service api, *ISPRS International Journal of Geo-Information* 11 (7) (2022) 394.
- [70] S. Sun, Q. Sun, F. Zhang, J. Ma, A spatial accessibility study of public hospitals: A multi-mode gravity-based two-step floating catchment area method, *Applied Sciences* 14 (17) (2024) 7713.
- [71] S. Guo, C. Song, T. Pei, Y. Liu, T. Ma, Y. Du, et al., Accessibility to urban parks for elderly residents: Perspectives from mobile phone data, *Landscape and Urban Planning* 191 (2019) 103642. doi:10.1016/j.landurbplan.2019.103642.

- [72] B. Tahmasbi, M. H. Mansourianfar, H. Haghshenas, I. Kim, Multimodal accessibility-based equity assessment of urban public facilities distribution, *Sustainable Cities and Society* 49 (2019) 101633.
- [73] L. Shi, Ü. Halik, A. Abliz, Z. Mamat, M. Welp, Urban green space accessibility and distribution equity in an arid oasis city: Urumqi, china, *Forests* 11 (6) (2020) 690. doi:10.3390/f11060690.
- [74] Associated Press, California wildfire triggers evacuations as homes burn and winds whip flames, accessed: 2025-04-03 (2025).
URL <https://apnews.com/article/california-wildfires-evacuation-alerts-69f10d320df14c6394fc2c646d1ff0ce>
- [75] Visit Pasadena, Visit pasadena - official visitor information, <https://www.visitpasadena.com/convention-center>, accessed: 2025-02-24 (n.d.).
- [76] Celery Octopus, Celery octopus - website, <https://celery-octopus-rx3m.squarespace.com/fairplex>, accessed: 2025-02-24 (n.d.).
- [77] Glendale Civic Center, Glendale civic center - venue information, <https://www.cvent.com/venues/glendale/8/glendale-civic-center/venue-180965f7-7a40-4dc0-8acf-dea65337a7bd>, accessed: 2025-02-24 (n.d.).